Available online at www.sciencedirect.com
ScienceDirect
Advances in Water Resources 31 (2008) 1137–1150
Advances in Water Resources
www.elsevier.com/locate/advwatres

Dimensional analysis of two-phase flow including a rate-dependent capillary pressure–saturation relationship

Sabine Manthey [a,*], S. Majid Hassanizadeh [b], Rainer Helmig [a], Rudolf Hilfer [c]

[a] Universität Stuttgart, Institute of Hydraulic Engineering, Research Group of Hydromechanics and Modelling of Hydrosystems, Pfaffenwaldring 61, 70569 Stuttgart, Germany
[b] University of Utrecht, Faculty of Geosciences, Environmental Hydrogeology Group, P.O. Box 80021, 3508 TA Utrecht, The Netherlands
[c] Universität Stuttgart, Institute of Computational Physics, Pfaffenwaldring 27, 70569 Stuttgart, Germany

Received 15 March 2007; received in revised form 4 December 2007; accepted 18 January 2008
Available online 10 March 2008

Abstract

The macroscopic modelling of two-phase flow processes in subsurface hydrosystems or industrial applications on the Darcy scale usually requires a constitutive relationship between capillary pressure and saturation, the $P_c(S_w)$ relationship. Traditionally, it is assumed that a unique relation between P_c and S_w exists independently of the flow conditions as long as hysteretic effects can be neglected. Recently, this assumption has been questioned and alternative formulations have been suggested. For example, the extended $P_c(S_w)$ relationship by Hassanizadeh and Gray [Hassanizadeh SM, Gray WG. Mechanics and thermodynamics of multiphase flow in porous media including interphase boundaries. Adv Water Resources 1990;13(4):169–86] proposes that the difference between the phase pressures to the equilibrium capillary pressure is a linear function of the rate of change of saturation, thereby introducing a constant of proportionality, the coefficient τ. It is desirable to identify cases where the extended relationship needs to be considered. Consequently, a dimensional analysis is performed on the basis of the two-phase balance equations. In addition to the well-known capillary and gravitational number, the dimensional analysis yields a new dimensionless number. The dynamic number Dy quantifies the ratio of dynamic capillary to viscous forces. Relating the dynamic to the capillary as well as the gravitational number gives the new numbers DyC and DyG, respectively. For given sets of fluid and porous medium parameters, the dimensionless numbers Dy and DyC are interpreted as functions of the characteristic length and flow velocity. The simulation of an imbibition process provides insight into the interpretation of the characteristic length scale. The most promising choice for this length scale seems to be the front width. We conclude that consideration of the extended $P_c(S_w)$ relationship may be important for porous media with high permeability, small entry pressure and high coefficient τ when systems with a small characteristic length (e.g. steep front) and small characteristic time scale are under investigation.

Keywords: Two-phase flow; Capillary pressure-saturation relationship; Rate dependence; Dimensional analysis; Dimensionless numbers

1. Introduction and motivation

Flow processes in porous media involving two immiscible fluids need to be understood and predicted when dealing with subsurface hydrosystems or industrial applications. For example, in the unsaturated zone, the spatial distribution of the water and air phase as well as their fluxes serve as a basis for modelling transport of contaminants such as pesticides or heavy metals (e.g. [9]). In the saturated zone, two-phase systems are encountered when non-aqueous phase liquids infiltrate into the subsurface. The simulation of these processes aids in advising remediation measures (see e.g. [37,49]). As examples for industrial applications in two-phase flow, the movement of fluids through a filter, concrete or moisture absorbents as well as the infiltration of ink into paper can be considered.

The physical–mathematical model underlying simulations of two-phase flow on the macro scale, here denoted

* Corresponding author.
E-mail address: sabine.manthey@iws.uni-stuttgart.de (S. Manthey).

0309-1708/$ - see front matter © 2008 Elsevier Ltd. All rights reserved.
doi:10.1016/j.advwatres.2008.01.021

Notation[1]

α	subscript: wetting or non-wetting phase
α^{VG}	Van Genuchten, 1980 parameter [Pa^{-1}]
α_S	Stauffer scaling parameter [–]
γ	interfacial tension [N/m]
Δt	time step [s]
θ	contact angle [°]
λ	Brooks and Corey parameter [–]
$\bar{\lambda}$	total mobility [$Pa^{-1}\ s^{-1}$]
μ	dynamic fluid viscosity [Pa s]
ϱ	density [kg/m^3]
ϱ_{IF}	mass of interface [$kg\ m^3$]
τ	damping coeffeficient [Pa s]
τ_B	coefficient after Barenblatt [s]
τ^*	coefficient after Bourgeat and Panfilov [–]
τ_{HG}	coefficient after Hassanizadeh and Gray [Pa s]
τ_K	coefficient after Kalaydjian [Pa s]
τ_S	coefficient after Stauffer [Pa s]
ϕ	porosity [–]
a	interfacial area per volume [m^{-1}]
f_w	fractional flow function [–]
d	pore diameter [m]
g	scalar gravitational acceleration [m/s^2]
h_{cr}	capillary rise [m]
K	scalar intrinsic permeability [m^2]
k_r	relative permeability [–]
l_c	characteristic length [m]
M_w^c	cumulative mass of wetting phase [kg]
P	pressure [Pa]
P_c	capillary pressure [Pa]
P_c^e	equilibrium capillary pressure [Pa]
P_c^d	dynamic capillary pressure [Pa]
P_{cc}	characteristic capillary pressure [Pa]
P_d	entry pressure for the $P_c(S_w)$ relationship after Brooks and Corey [Pa]
R	radius [m]
S	saturation [–]
$S_{\alpha r}$	residual saturation of phase α [–]
S_e	effective saturation of the wetting phase [–]
T	temperature [K]
t	time [s]
t_c	characteristic time [s]
v	Darcy velocity [m/s]
u_s	seepage velocity [m/s]
V	volume [m^3]
z	depth [m]

[1] Note: Local notations are explained in the text. Vectors and matrices are written in bold type. Averaged values are marked with $\langle\rangle$.

as Darcy scale, usually requires a constitutive relationship between wetting phase (denoted by subscript w) saturation S_w and capillary pressure P_c; the $P_c(S_w)$ relationship. Traditionally, one assumes that this relationship is determined under quasi-static or steady-state conditions but can be applied to any transient flow process that fulfills the Reynolds number criterion (i.e. $\varrho_w u_s d/\mu_w < 1$). However, recently some works have questioned this assumption (see e.g. [14] or [33]). [35] were able to improve the agreement between experimental and simulation results by applying a model which accounts for a rate dependence in the $P_c(S_w)$ relationship. Although recently rate dependence in the $P_c(S_w)$ relationship has attracted some attention, the importance of including such a relationship in simulations still needs to be identified. One may safely assume that for slow flow processes (e.g. small capillary number) a rate-dependent relationship does not need to be accounted for. But, it is not clear under what conditions such effects may be important. In order to identify the relevant flow regimes and to obtain quantitative measures, we will here perform a dimensional analysis of the two-phase balance equations with a rate-dependent $P_c(S_w)$ relationship. For a dimensional analysis of the two-phase balance equations including the traditional $P_c(S_w)$ relationship, the works of [22,24,1], or, for heterogeneous systems, [23] can be consulted.

This paper is structured as follows. We first describe when and why rate dependence in the $P_c(S_w)$ relationship may be observable and then shortly review different models accounting for the rate dependence. These models will in the following also be referred to as extended models. Then the physical–mathematical model of two-phase flow is introduced. Within a dimensional analysis the balance equations are non-dimensionalised by introducing characteristic and dimensionless magnitudes. Resulting from the analysis, dimensionless numbers can be defined. It is assumed then, that these numbers can be consulted to assess the relative importance of the different dimensionless terms in the balance equations. The magnitude of the numbers is thus calculated for some soils. They are then interpreted as functions of the characteristic length scale or velocity. In order to test the suggested interpretations of the characteristic length simulations of an imbibition process are carried out. For these simulations the dimensionless numbers are calculated. Finally, it is assessed when the consideration of an extended $P_c(S_w)$ relationship may be of importance.

2. Rate-dependent effects in the $P_c(S_w)$ relationship

Laboratory experiments have shown that the relationship between capillary pressure and saturation might not

be unique. Well-known effects are for example the hysteretic behaviour of the relation or the entry pressure, which needs to be attained before non-wetting phase can infiltrate into the porous medium. Also, a rate dependence has been observed, here denoted as dynamic effect.

Traditionally, a $P_c(S_w)$ relationship is determined under quasi-static or steady-state conditions (for example with a pressure cell or a centrifuge, see [10]). This capillary pressure is here addressed as equilibrium capillary pressure P_c^e and the relation thus as equilibrium $P_c^e(S_w)$ relationship. It is assumed to be unique as long as hysteresis can be neglected (in the Brooks and Corey [8] $P_c(S_w)$ relationship a non-uniqueness also exists at $S_w = 1.0$). Under transient conditions when the rate of change of saturation well exceeds zero, the dynamic capillary pressure P_c^d prevails resulting in a dynamic $P_c^d(S_w)$ relationship. In the following, the term 'rate of change of saturation' will be abbreviated to 'saturation rate'. Instead of measuring P_c and S_w at given equilibrium distributions of the phases, they are determined continuously over time as the flow occurs. For a given porous medium, in theory an infinite number of dynamic $P_c(S_w)$ relationships could be measured for varying flow conditions. This leads to a non-uniqueness in the relation between capillary pressure and saturation. For illustration, the equilibrium and dynamic $P_c(S_w)$ relationships obtained in experiments by [41] are depicted (see Fig. 1).

Many authors give physical explanations for the occurrence of dynamic effects. [16,50] summarise the literature, as well as [18]. The summaries are shortly reproduced here including additional remarks.

On the pore scale, the dynamic contact angle is often given as one reason for the dynamic effect in capillary pressure. The contact angle decreases with increasing flow velocity for drainage and increases with increasing velocity

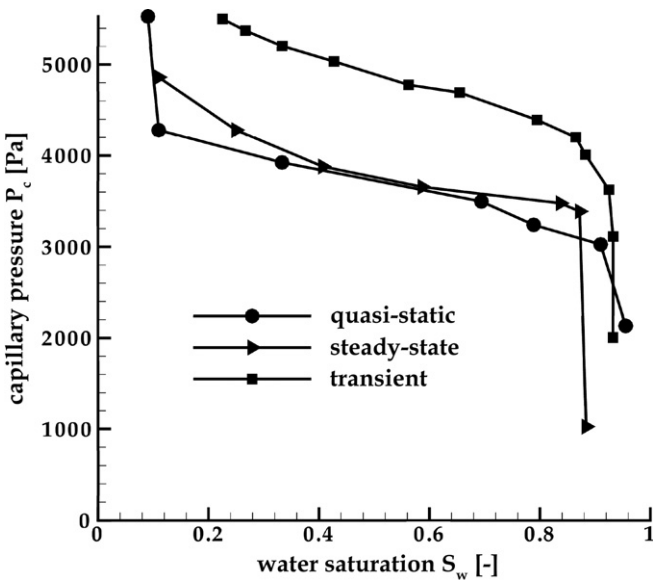

Fig. 1. Illustration of dynamic effects in drainage $P_c(S_w)$ relationships with experimental results from Topp et al. [41].

for imbibition (see e.g. [6,15,48]). Consequently, capillary pressure for drainage is higher than equilibrium capillary pressure, while for imbibition it is lower.

For imbibition, the following processes have been identified. [4] argue that, for imbibition processes, the non-sequential filling of pores by the wetting fluid may cause dynamic effects. With non-sequential filling they define a filling of pores with water in an order that would not be predicted applying the Young–Laplace equation. On the basis of this equation one can calculate up to which pore diameter pores would be imbibed with water for a given (equilibrium) capillary pressure. However, [4] assume that under dynamic conditions also a pore with a larger diameter might be wetted with water. If the diameter of this pore is then inserted into the Young–Laplace equation the (dynamic) P_c calculated with this diameter would be smaller than the given equilibrium one.

Moreover, in dynamic imbibition processes, enhanced air entrapment can result in an increase in the residual non-wetting phase (subscript n) saturation S_{nr} compared to the equilibrium $P_c^e(S_w)$ relationship. Consequently, at a given saturation, a lower capillary pressure for the dynamic case as opposed to the equilibrium one, can be observed (e.g. [13]). This assumes that the entrapped non-wetting phase does not contribute to the capillary pressure or that within the entrapped phase the same pressure prevails as in the continuous non-wetting phase. Obviously, dynamic and hysteretic effects are confounded here. It is assumed that such pore-scale processes might result in hysteretic as well as dynamic effects.

Related to the experimental set up and problems of inverse parameter identification, the following aspects deserve attention. Water can be drained only if air can infiltrate the porous medium at the same time. If air access is limited, higher water saturations might occur under dynamic conditions. Especially, [43,39] point out that the dynamic effect in the $P_c(S_w)$ relationship is not pronounced if the drainage experiment is conducted with a column possessing perforated walls which ensure air access into the column. Moreover, several authors have shown that air pressure does not always equal atmospheric pressure during laboratory experiments and that thus the capillary pressure derived from tensiometer measurements is misleading (e.g. [27,39,47]).

The first one known to the authors to propose an (empirical) relationship was Stauffer [40]. He examined one-dimensional vertical drainage processes in three fine sand columns with water and gas (air) as fluids. In search of a functional relationship to account for non-uniqueness in the $P_c(S_w)$ relationship he plotted the difference between the dynamic and the equilibrium capillary pressure as a function of (a) the rate of change of saturation and (b) the rate of change of capillary pressure. While the relationship in the first case seemed to be linear, it appeared to be non-linear in the second case. Stauffer [40] chose to concentrate on the linear dependence, proposing the empirical relationship

$$P_c^d - P_c^e(S_w) = -\tau_S \frac{\partial S_w}{\partial t}, \quad (1)$$

with the coefficient τ_S defined by

$$\tau_S = \frac{\alpha_S \mu_w \phi}{K\lambda}\left(\frac{P_d}{\varrho_w g}\right)^2, \quad (2)$$

where $\alpha_S = 0.1$ denotes a constant scaling parameter, μ_w the viscosity of the wetting phase, ϕ the porosity, K the intrinsic permeability, ϱ_w the density of the wetting phase, g the gravitational constant and P_d, λ stem from the Brooks and Corey [8] parametrisation. The coefficient τ_S $[ML^{-1}T^{-1}]$ can thus be calculated for a given porous medium containing water and air. The dynamic capillary pressure P_c^d in Eq. (1) can be expressed as the difference in the phase pressures $P_n - P_w$, which only equals the equilibrium capillary pressure under static or steady-state conditions.

All other alternative formulations of dynamic capillary pressure are based on theoretical considerations. Kalaydjian [25] sets up macroscopic balance equations of mass, momentum, energy and entropy for two incompressible, immiscible fluid phases and their interfaces as well as phenomenological equations on the basis of the theory of irreversible thermodynamic processes. Expressed in terms of the wetting phase for a rigid porous medium, Kalaydjian [25] proposes the relation

$$P_n - P_w - \frac{2}{R}\gamma = -\tau_K \phi \frac{\partial S_w}{\partial t}. \quad (3)$$

Here, R is the pore radius and γ the interfacial tension. In this model, it is assumed that at equilibrium the interface between the wetting and the non-wetting phase is hemispherical, which presumes a circular cross section of all pores. The left hand side can be interpreted as the difference between dynamic capillary pressure, $P_c^d = P_n - P_w$, and the equilibrium capillary pressure. Thus, although Kalaydjian's model can strictly speaking only be employed for porous media with cylindrical pores, with the interpretations just given it resembles Eq. (1) by Stauffer [40]. In an experimental investigation Kalaydjian [26] shows his τ parameter to be a function of the effective water saturation and of the inflow rate of wetting phase which can be interpreted as a functional dependence on the rate of change of saturation. However, he does not attempt to find a functional form for the in one case convex and in the other case concave data points $\tau(S_e)$ of the two imbibition experiments.

Barenblatt and co-workers set up their model in [3], and further developed it in [2] as well as [4]. The authors devise a model for describing non-equilibrium effects for water–oil displacement or spontaneous countercurrent imbibition processes. While assuming that the equilibrium $P_c(S_w)$ relationship still holds, the authors propose that it should not be evaluated at the actual wetting phase saturation occurring in the system but at an apparent saturation η. For an imbibition process the apparent wetting phase saturation can be higher than (or equal to) the actual saturation. Barenblatt et al. [4] suggest an empirical relation between the apparent and the actual saturation S_w

$$\eta - S_w = \tau_B \frac{\partial S_w}{\partial t}, \quad (4)$$

where τ_B [T] denotes a constant redistribution time. Note, that thus this parameter has a different unit compared to the ones from the other models described here.

Hassanizadeh and Gray [19] have volume-averaged the pore-scale balance equations of mass, momentum, energy and entropy and have applied the concept of the entropy inequality. They propose an alternative formulation of the $P_c(S_w)$ relationship similar to that of [40,25], namely that the difference between the non-wetting phase pressure P_n, the wetting phase pressure P_w and the equilibrium capillary pressure P_c^e is a linear function of the rate of change of wetting phase saturation

$$P_n - P_w - P_c^e(S_w) = -\tau_{HG} \frac{\partial S_w}{\partial t}, \quad \text{with} \quad (5)$$

$$\tau_{HG} = f(\varrho_\alpha, \phi, S_w, a, \varrho_{IF}, T), \quad (6)$$

where ϱ_α denotes the mass of a phase, a denotes the interfacial area per volume, ϱ_{IF} the mass allocated to the interface, and T is the temperature. So far, to our knowledge only the functional dependence on water saturation has been studied in laboratory experiments.

The model of Hassanizadeh and Gray was applied by several authors for theoretical investigations of the flow of water–air or two-phase flow. Nieber et al. [33] incorporated the extended $P_c(S_w)$ dependence into the Richards equation in order to analyse instabilities in gravity-driven flow. They assume that τ can be factorised into a constant part, a part that is a function of water saturation and a part that is a function of water pressure. They point out that a number of functions could be applied and choose power functions for both dependencies. Moreover, Cuesta et al. [11] and van Duijn et al. [44] have also analysed travelling wave solutions for the Richards equation and the two-phase balance equations respectively. They assume that τ is a (power) function of water saturation.

O'Carroll et al. [35] have calculated the τ parameter after Hassanizadeh and Gray with inverse parameter identification on the basis of multi-step outflow experiments employing water and tetrachlorethene. They attained the best fit by assuming a linear dependence of τ on the effective water saturation S_e with $\tau(S_e = 1.0) = 0$.

As the functional choice for $\tau(S_w)$ of most of these authors is mainly motivated by mathematical considerations and only few physical experiments exist we detain here from choosing one of the functional dependencies of the coefficient τ on the water saturation.

In the following analysis, we restrict our study to the following linear model proposed by Stauffer [40], Kalaydjian [25] and Hassanizadeh and Gray [19]

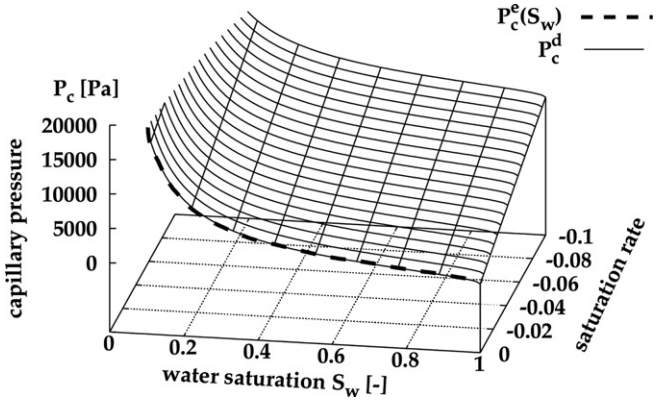

Fig. 2. Example plot of the extended $P_c(S_w)$ relationship $P_c^d = -\tau\partial S_w/\partial t + P_c^e$ for drainage and a constant $\tau = 10^5$ Pa s.

$$P_n - P_w - P_c^e(S_w) = P_c^d - P_c^e(S_w) = -\tau\frac{\partial S_w}{\partial t}, \tag{7}$$

where τ is assumed to be a constant. We make this assumption as the functional dependencies of τ and especially the functional relationship with water saturation have not been established clearly yet. We will refer back to this issue in the section on the dimensional analysis.

Eq. (7) predicts that the phase pressure difference (interpreted here as the dynamic capillary pressure) equals the equilibrium capillary pressure at a given water saturation only under static or steady-state conditions. For transient flow conditions, the difference between the two capillary pressures depends on the magnitude of the saturation rate and the coefficient τ. The extended relationship is illustrated in Fig. 2.

In the following, the extended $P_c(S_w)$ relationship given by Eq. (7) will be applied to close the conservation equations for two-phase flow in porous media.

3. Physical–mathematical model of two-phase flow processes

For the mathematical description of two-phase flow, the conservation equations of mass and momentum are employed. The two fluid phases and the porous medium are assumed to be incompressible. The porous medium is considered to be isotropic. For the momentum balance the Darcy law extended to multi-phase flow is employed. Using the additional constraint

$$S_w + S_n = 1, \tag{8}$$

and by applying the extended $P_c(S_w)$ relationship as closure assumption, the four primary variables P_w, P_n, S_w, S_n can be reduced to two, e.g. the saturation of the non-wetting phase and the pressure of the wetting phase. Inserting Darcy's law into the mass balance equations, these can be formulated for the wetting as

$$-\phi\frac{\partial S_n}{\partial t} - \nabla\cdot\left\{\frac{k_{rw}(1.0 - S_n)}{\mu_w}K\nabla(P_w - \varrho_w g z)\right\} = 0, \tag{9}$$

and the non-wetting phase as

$$\phi\frac{\partial S_n}{\partial t} - \nabla\cdot\left\{\frac{k_{rn}(S_n)}{\mu_n}K\nabla(P_w + P_c + \tau\frac{\partial S_n}{\partial t} - \varrho_n g z)\right\} = 0. \tag{10}$$

In these balance equations $k_{r\alpha}$ denotes the relative permeability of phase α, which is a function of its saturation. It is assumed that source/sink terms do not occur and that z is positive downward.

4. Dimensional analysis

The dimensional analysis is performed here on the basis of the two balance Eqs. (9) and (10), where a rate dependence in the $P_c(S_w)$ relationship is accounted for. The balance equations are non-dimensionalised by introducing the following dimensionless and characteristic magnitudes:

$$z = l_c\hat{z}, \tag{11}$$

$$\nabla = \widehat{\nabla}/l_c, \tag{12}$$

$$t = t_c\hat{t}, \quad \text{with } t_c = \phi l_c/u_c \quad \text{and} \tag{13}$$

$$P_\alpha = P_{cc}\widehat{P_\alpha}, \quad \text{with } \alpha \in \{w, c\}. \tag{14}$$

Dimensionless quantities are marked with a hat, and the subscript c denotes a characteristic magnitude. The characteristic time, length and flow velocity are related through Eq. (13), thus only two of them can be chosen independently. For non-dimensionalising the pressures, a characteristic capillary pressure, P_{cc}, is applied. It can be based on the equilibrium $P_c^e(S_w)$ relationship of the porous medium under consideration, using e.g. the capillary pressure at a medium effective water saturation [1]. In case the van Genuchten parameterisation is applied one could employ the inverse of the parameter α^{VG} in units of pressure. Also, the entry pressure P_d appearing as a parameter in the Brooks and Corey parameterisation suggests itself. An interpretation of the characteristic length and time will be given later on. It should be stressed here that usually one only employs a single value for each of the characteristic quantities. However, in reality we mostly deal with transient processes (especially here, where the importance of dynamic effects should be estimated). As a consequence, one should keep in mind that the relative value of the forces will only be estimated but not be calculated exactly for a whole transient process at all locations in a given system.

With the definitions given in Eq. (11) to Eq. (14), the balance Eqs. (9) and (10) can be reformulated as

$$-\frac{\partial S_n}{\partial\hat{t}} = \widehat{\nabla}\cdot\left\{k_{rw}(1.0 - S_n)\left[\frac{KP_{cc}t_c}{\mu_w l_c^2\phi}\widehat{\nabla}\widehat{P_w} - \frac{K\varrho_w g t_c}{\mu_w l_c\phi}\widehat{\nabla}\hat{z}\right]\right\}, \tag{15}$$

and

$$\frac{\partial S_n}{\partial \hat{t}} = \widehat{\nabla}\cdot\left\{k_{rn}(S_n)\frac{\mu_w}{\mu_n}\left[\frac{KP_{cc}t_c}{\mu_w l_c^2\phi}(\widehat{\nabla}\widehat{P_w}+\widehat{\nabla}\widehat{P_c})\right.\right.$$
$$\left.\left.+\frac{K\tau}{\mu_w l_c^2\phi}\widehat{\nabla}\frac{\partial S_n}{\partial \hat{t}}-\frac{\varrho_n}{\varrho_w}\frac{K\varrho_w g t_c}{\mu_w l_c\phi}\widehat{\nabla}\hat{z}\right]\right\}. \quad (16)$$

The ratios of the flux term in Eq. (16) were extended by the viscosity ratio and the density ratio respectively to receive the same dimensionless numbers in both balance equations. As a consequence, comparisons are facilitated and one only needs to assess three instead of five dimensionless numbers.

Traditionally, the ratio of viscous to capillary forces is referred to as the capillary number. However, we here define the capillary number as the ratio of capillary to viscous force. Then, as a consequence, its interpretation is more intuitive: For a large capillary number, capillary forces dominate, as the name would suggest. The capillary number is thus defined to be

$$\mathrm{Ca} = \frac{KP_{cc}t_c}{\mu_w l_c^2\phi} = \frac{KP_{cc}}{\mu_w u_c l_c} = \frac{\text{equilibrium capillary force}}{\text{viscous force}}. \quad (17)$$

As the capillary number also arises in the dimensionless balance equations if a traditional $P_c^e(S_w)$ relationship is employed to close the system of equations, the capillary forces are denoted here equilibrium capillary forces. Next, the gravity number as traditionally defined is given by

$$\mathrm{Gr} = \frac{K\varrho_w g t_c}{\mu_w l_c\phi} = \frac{K\varrho_w g}{\mu_w u_c} = \frac{\text{gravitational force}}{\text{viscous force}}. \quad (18)$$

Note, that while the enumerator and denominator of the capillary number have the units of a force, in the gravity number they have force per length and would need to be extended by the characteristic length in order to regain a force.

In addition to these well-known dimensionless numbers, a new factor appears in Eq. (16). This factor is related to the gradient of the rate of change of saturation. We refer to it as the 'dynamic number' and define it as

$$\mathrm{Dy} = \frac{K\tau}{\mu_w l_c^2\phi} = \frac{\text{dynamic capillary force}}{\text{viscous force}}. \quad (19)$$

Both parts of the ratio need to be extended by the inverse of characteristic time to obtain a force. The number Dy resembles the dimensionless grouping employed by Dahle et al. [12], who analysed the behaviour of the coefficient τ derived from computations of flow in a bundle of capillary tubes.

We here have made the assumption that capillary forces can be divided into forces determined by the equilibrium $P_c(S_w)$ relationship and the ones stemming from dynamic effects in capillary pressure. Moreover, we presume that the dynamic effects in the capillary pressure are captured by the τ coefficient. As the parameter τ has the same units as the dynamic viscosity, a different interpretation of the numerator could be an 'apparent viscosity'. Assuming that at least a part of the dynamic effects in the capillary pressure can be ascribed to viscous forces, this interpretation could perhaps capture the physical origins of dynamic effects well. However, as the effects can only occur in a multi-phase system where capillary forces play a role we will here adhere to the term dynamic capillary force bearing in mind that the effects might be a mixture of viscous and capillary forces. The dimensionless balance equations can now be formulated as

$$-\frac{\partial S_n}{\partial \hat{t}} = \widehat{\nabla}\cdot\{k_{rw}(1.0-S_n)(\mathrm{Ca}\widehat{\nabla}\widehat{P_w}-\mathrm{Gr}\widehat{\nabla}\hat{z})\}, \quad (20)$$

and

$$\frac{\partial S_n}{\partial \hat{t}} = \widehat{\nabla}\cdot\left\{k_{rn}(S_n)\frac{\mu_w}{\mu_n}\left[\mathrm{Ca}(\widehat{\nabla}\widehat{P_w}+\widehat{\nabla}\widehat{P_c})\right.\right.$$
$$\left.\left.+\mathrm{Dy}\,\widehat{\nabla}\frac{\partial S_n}{\partial \hat{t}}-\frac{\varrho_n}{\varrho_w}\mathrm{Gr}\,\widehat{\nabla}\hat{z}\right]\right\}. \quad (21)$$

Further insight can be gained by relating the various dimensionless numbers. Thus, the ratio of the dynamic number to the capillary number yields the dimensionless number DyC

$$\mathrm{DyC} = \frac{\mathrm{Dy}}{\mathrm{Ca}} = \frac{K\tau}{\mu_w l_c^2\phi}\frac{\mu_w u_c l_c}{KP_{cc}} = \frac{u_c\tau}{P_{cc}l_c\phi}$$
$$= \frac{\text{dynamic capillary force}}{\text{equilibrium capillary force}}. \quad (22)$$

Again, the number needs to be extended by l_c/l_c in order to obtain forces. The new number DyC includes the characteristic flow velocity, which is to be expected to some extent. One should be careful though, as the flow velocity is not necessarily related to the rate of change of saturation as it also occurs under steady-state conditions (in which case the saturation rate goes to zero). In the framework of this dimensional analysis, it is thus required that the characteristic flow velocity can be connected to a transient process because otherwise the whole dynamic term would vanish. Obviously, in a transient process the flow velocity changes and thus the dimensional analysis can only give an estimation of the dominating forces for a given point in time. We propose here to use the maximum flow velocity, as this should for a transient flow process relate to the maximum saturation change and thus should be the upper bound for the importance of dynamic effects (assuming that τ is a constant).

If the characteristic velocity u_c in Eq. (22) is replaced by $u_c = \phi l_c/t_c$, DyC becomes

$$\mathrm{DyC} = \frac{\tau}{t_c P_{cc}}. \quad (23)$$

With this reformulation, one may conclude that the influence from the dynamic effects is large for small time scales or small characteristic equilibrium capillary pressures.

Similar to the number DyC, one may define a dimensionless number DyG as the ratio of Dy to Gr,

$$\mathrm{DyG} = \frac{\mathrm{Dy}}{\mathrm{Gr}} = \frac{K\tau}{\phi\mu_w l_c^2}\frac{\mu_w u_c}{K\varrho_w g} = \frac{\tau u_c}{\phi l_c^2\varrho_w g}$$
$$= \frac{\text{dynamic capillary force}}{\text{gravitational force}}. \quad (24)$$

This number indicates that the influence of dynamic capillary forces decreases with the characteristic length scale in relation to the gravitational forces.

As described above, some authors have suggested functional dependencies for the τ coefficient, e.g. a dependence on the water saturation. A functional dependence could be introduced by splitting τ into a characteristic constant τ_c (equivalent to using the characteristic capillary pressure) and a dimensionless part $\widehat{\tau}(S_w,\ldots)$ that describes the dependencies. As a consequence of the fractionalisation, τ_c instead of τ enters into the dimensionless number Dy and the dimensionless part could be treated as an additional factor. It should be stressed here though that for a complete assessment of the system the whole dimensionless balance equations need to be considered (including initial and boundary conditions), which contain non-linear parts depending on the (with time varying) saturation. We here have a different aim. We would like to provide the reader with a tool for a rule-of-thumb assessment of the dominating forces of a system. This assessment should help to simplify the to be solved balance equations by neglecting terms (e.g. the gravity term or the dynamic term). For this rule-of-thumb assessment choices need to be made for the characteristic magnitudes. For the following analysis we thus assume a constant τ parameter.

In the following, some exemplary calculations of the dimensionless numbers are presented with a view to providing insight and interpretation of the numbers. In order to accurately assess the influence of the different terms within the system the products of the dimensionless numbers and the dimensionless gradients need to be considered. Also, not only the two balance equations would need to be non-dimensionalised but also the initial and boundary conditions. However, if only the fluid and porous medium parameters are known in advance, a calculation of the dimensionless numbers could give a first insight as to the relative importance of the forces. In the following, we thus assume that either we have only a sparse knowledge of the system and lack the exact magnitude of the dimensionless gradients. Or, the characteristic magnitudes are chosen such that all dimensionless gradients scale on the same order of magnitude. In the latter case a comparison of the dimensionless numbers alone would suffice to assess the dominating forces.

5. Analytical computations

In this section, we employ the definitions of the dimensionless numbers to find out about the relative significance of various forces for different flow regimes. Assuming that the properties of the homogeneous porous medium are known and constant on all length scales, the dimensionless numbers can be interpreted as functions of characteristic flow velocity, characteristic time, or characteristic length. As mentioned before these three characteristic magnitudes are related through Eq. (13), leaving two of them independent. The choice of these characteristic parameters depends on the process. For the following interpretation, the characteristic flow velocity and length scale are considered independently of each other. While the characteristic flow velocity can be determined easily by using either a maximum or average flow velocity expected for the system under consideration, it is open to discussion yet how the characteristic length should be defined. This question will be tackled later in this section.

For the following analysis, it is assumed that the parameters are known and constant for a given porous medium. Whereas the methods to evaluate parameters like the permeability or the equilibrium $P_c(S_w)$ relationship have been developed for decades, the determination of the coefficient τ is at early stages yet. There exist laboratory and numerical works. Several laboratory experiments were analysed by Hassanizadeh et al. [18], who on that basis calculated a range of τ values from data published in the literature. These experiments were not aimed at the determination of τ but provided measurements (indirect and direct) of equilibrium and dynamic $P_c(S_w)$ relationships as well as data with which the rate of change of saturation could be estimated. Using linear regression on the basis of Eq. (7) Hassanizadeh et al. were then able to determine the τ coefficient. Oung et al. [36], Hassanizadeh et al. [20], Manthey et al. [31] and Bottero et al. [7] have also calculated the coefficient from directly measured $P_c^e(S_w)$ and $P_c^d(S_w)$ relationships and the saturation rates by performing linear regression. O'Carroll et al. [35] have calculated the parameter with inverse parameter identification using a multi-step outflow experiment. Some of these data will be used here.

Moreover, numerical works exist where the coefficient τ was calculated by means of numerical experiments with a bundle of tube model [12], a pore-network model [17] and a Darcy scale model [30]. In all of the above mentioned works, the parameter τ was shown to depend on the averaging length scale which might be due to the way the phase pressures were averaged. In the meantime, the work of Nordbotten et al. [34] has shown that the averaging of the phase pressures as done in the above mentioned works leads to inconsistencies in the upscaled balance equations. As long as the question of how to correctly determine average phase pressures has not been resolved we abstain here from applying the averaging length-dependent τ values from the numerical works.

As mentioned in Section 1, Stauffer [40] proposed the formula given in Eq. (2) to relate τ to system properties. Table 1 lists the τ_S values for five different soil types which were calculated using this formula. For the Zeijen sand (ZS), the Baskarp sand (BS), and 'Sand 1' also τ values from the literature are available. These are based on laboratory experiments.

The Stauffer formula can also be employed to obtain a dimensionless number Dy in which τ does not occur. Such a number would be useful as at the moment only few laboratory experiments are available where τ was determined. Substitution of Eq. (2) in Eq. (19) results in a relationship for the number Dy that is independent of the parameter τ,

Table 1
Porous media parameters, τ_S after Eq. (2), $\tau_{Exp.}$ from experimental data

Soil type	K (m^2)	ϕ (–)	P_d (Pa)	λ (–)	τ_S (Pa s)	$\tau_{Exp.}$ (Pa s)
CS	5.66×10^{-11}	0.32	1370	5.83	1.89×10^3	–
Sand 1	2×10^{-12}	0.37	2805	7.18	2×10^5	2×10^7
ZS	3.06×10^{-12}	0.35	5587	6.11	6.07×10^5	$2.0 \times 10^5 (S_w = 0.6)$
BS	5.7×10^{-12}	0.35	3800	0.161	6.4×10^6	0 to 5.9×10^5
Silt	5.16×10^{-13}	0.49	9412	0.56	1.56×10^8	–

Parameter for CS from [42] Brooks and Corey parameters derived after Lenhard et al. [28], Sand 1 from Topp et al. [41] P_d from $P_c(S_w)$ plot, K from grain size distribution (Bialas and Kleczkowski [5] and Hassanizadeh et al. [18], ZS from Hassanizadeh et al. [20] and Bottero et al. [7]), BS from Oung et al. [36] assuming that τ is given there in [kPa s] and permeability in [m/s], for Silt from Van Genuchten et al. [46].

$$\mathrm{Dy} = \frac{\alpha_S}{\lambda l_c^2}\left(\frac{P_d}{\varrho_w g}\right)^2, \tag{25}$$

where $P_d = P_{cc}$. Consequently, only the fluid properties and the Brooks and Corey parameters of the equilibrium $P_c(S_w)$ relationship would be required to assess the magnitude of Dy. However, in this reformulation no process-dependent magnitudes occur. This makes its application doubtful. The definition of Dy in Eq. (25) implies that if all other parameters remain constant, for fine porous media with a high entry pressure, dynamic effects are of importance and should thus be taken into account for any process. This is a consequence that still needs to be verified. It is not supported by the dimensionless analysis presented here.

To get an impression of the significance of dynamic effects, Eqs. (19) and (22) are employed to plot the dimensionless numbers Dy and DyC against the characteristic length l_c for Sand 1 and Zeijen sand ZS employing a characteristic velocity of $u_c = 10^{-5}$ m/s (see Fig. 3). These two sands were chosen as their τ values were determined on the basis of laboratory experiments.

The dimensionless number Dy quantifies the ratio of dynamic capillary to viscous forces. Dy decreases with increasing characteristic length, as the viscous force depends on length scale and thus dominates the dynamic capillary effect on large scales.

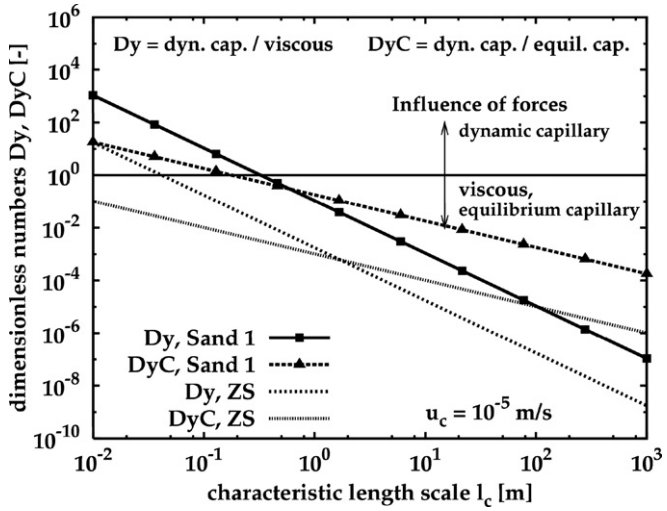

Fig. 3. Dimensionless numbers Dy and DyC as functions of the characteristic length scale for the Zeijen sand ZS and Sand 1 for $u_c = 10^{-5}$ ms (for the parameters: $P_{cc} = P_d$, $\tau = \tau_{Exp.}$, see Table 1).

The dimensionless number DyC relates the influence of the dynamic to the equilibrium capillary effects. With increasing length scale, the dynamic forces diminish in importance (see Fig. 3). For decreasing values of DyC, the equilibrium capillary pressure gains influence. For Sand 1, the balance of these two effects is attained at a length scale of $l \approx 0.2$ m; for the Zeijen sand, the length is about two orders of magnitude smaller.

As mentioned before, the characteristic length can be interpreted in different ways, e.g. as

- the system length,
- the characteristic length of a process, e.g. a front width, or as
- a property of the porous medium, e.g. the capillary rise or a representative pore diameter.

If the characteristic length is interpreted as the system length, then the dynamic capillary effect is important only on small scales (e.g. a small soil column experiment). For very small length scales the validity of the underlying Darcy law might be questioned as we then approach the pore scale where a different set of balance equations should be employed. If the characteristic length is interpreted as the length of the system under investigation, one should keep in mind that the dimensional analysis performed should not be applied for large length scales as on larger scales the porous medium is clearly heterogeneous. However, for the analysis here homogeneity of the porous medium was presumed. An advantage of using the system length is that it is a well-known magnitude. A disadvantage is that it does not relate to the real physical processes. These statements are valid vice versa for the front width.

For the front width as the characteristic length the upper bound is represented by the largest width of a front. For the lower bound, an REV again needs to be establishable, because the front is otherwise reduced to the pore-scale interface between the two phases. For the prediction of the front width the saturation formulation of the two-phase flow equations could be employed [21]

$$\nabla \cdot \left[\bar{\lambda} \mathrm{d}P_c/\mathrm{d}S_w \nabla S_w\right] = \left[v_t \mathrm{d}f_w/\mathrm{d}S_w\right]\nabla S_w, \tag{26}$$

where we neglect gravity effects as well as the accumulation term and assume that there are no sources/sinks. In Eq. (26) v_t denotes the total velocity $v_t = v_w + v_n$ and $\bar{\lambda}$ the total mobility after

$$\bar{\lambda} = \frac{\lambda_w \lambda_n}{\lambda_w + \lambda_n}, \tag{27}$$

where $\lambda_\alpha = k_{r\alpha}/\mu_\alpha$ is the mobility of phase α. Moreover, f_w denotes the fractional flow function

$$f_w = \frac{\lambda_w}{\lambda_w + \lambda_n}. \tag{28}$$

Approximating the spatial derivatives using $\Delta l = 1/l_c$ and recasting Eq. (26) leads to

$$l_c = \frac{\bar{\lambda}|dP_c/dS_w|}{v_t df_w/dS}. \tag{29}$$

In order to obtain a positive length the norm of the $P_c(S_w)$ derivative needs to be applied. The front width would thus be derived from a ratio quantifying the diffusive to the convective flux. In the limit of purely advective flow, the front width reduces to zero. In the case of a purely diffusion dominated process the front width goes to infinity. Then the system length should be chosen as the characteristic length. Disadvantage of this definition are that (a) the total velocity needs to be assessed a priori and (b) that three non-linear functions of the wetting phase saturation, namely the $P_c(S_w)$ relationship, total mobility and the fractional flow function enter into the l_c calculation. We suggest to evaluate the functions at a medium effective water saturation. Applying Eq. (29) for the estimation of the characteristic length has the advantage that both porous media properties (the derivative of the $P_c(S_w)$ relationship) and the influence from the process, namely the ratio of the diffusive to the advective flux enter into the calculation.

As properties of the porous medium the capillary rise

$$l_c = h_{cr} = P_{cc}/\varrho_w g, \tag{30}$$

or a representative pore diameter d relating to the square root of the intrinsic permeability (as we work on the Darcy scale)

$$l_c = d = 2 \cdot \sqrt{8K/\phi} \tag{31}$$

could be applied.These parameters should be known in advance, thus a characteristic length can be easily calculated. However, any influence of the process is not captured. Also, non-dimensionalising the gradients in the balance equations with a pore diameter might not seem appropriate as scale issues are confounded.

In the next section, we will apply the different suggested ways to calculate the characteristic length using a numerical simulation of an imbibition process.

Next, a constant length scale is chosen and the characteristic flow velocity is varied. For illustration, the calculated DyC is plotted for the parameters of the coarse sand CS and the Zeijen sand ZS (see Fig. 4).

For increasing flow velocities, the dynamic capillary force gains importance in relation to the equilibrium force. As an example, for the coarse sand CS, and for $l_c = 0.01$ m, the balance between dynamic and equilibrium capillary effects is attained at a characteristic flow velocity of appr. $u_c = 0.002$ m/s. For the Zeijen sand, the flow velocity at balance is approximately two orders of magnitude smaller for the same characteristic length.

The applicability of Darcy's law might be questionable at high flow velocities, as the linear relation of flux to head gradient can change to non-linear. As a measure, the Reynolds number is employed, which should not exceed unity for Darcy's law to hold. The characteristic flow velocity u_c can be related to the characteristic seepage velocity u_{sc} used in the Reynolds number through $u_{sc} = u_c/\phi$. As the dimensionless numbers are defined related to the wetting phase properties, the wetting phase parameters are employed. For reference, $Re_w(u_c = u_{sc}\phi) = 1$ is indicated in Fig. 4 for both sands. Apparently, for the Zeijen sand ZS, the range of velocities where dynamic forces dominate

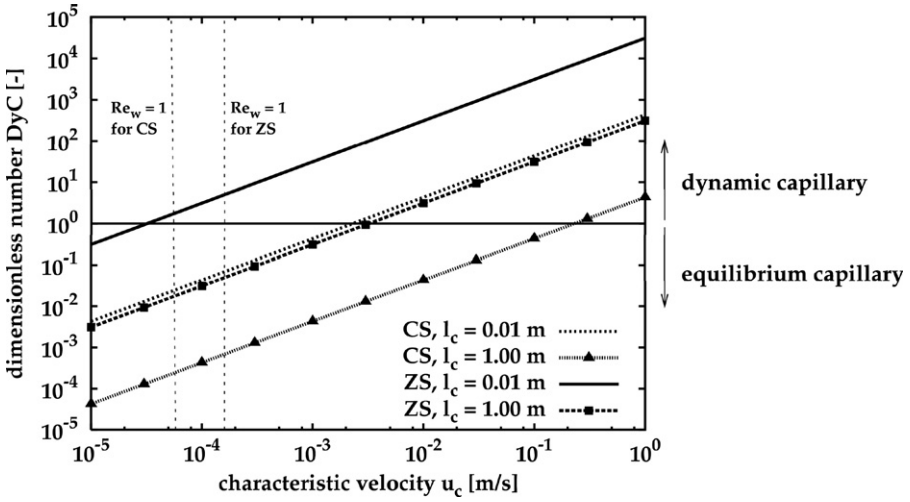

Fig. 4. Dimensionless number DyC as a function of the characteristic flow velocity for the coarse sand CS and the Zeijen sand ZS.

(DyC > 1) and the Darcy law holds, is very small for the characteristic length scale of $l_c = 0.01$ m. At the larger characteristic length the equilibrium capillary forces dominate throughout the whole range of the applicability of Darcy's law for the coarse sand CS and the Zeijen sand (ZS).

In the following, simulations are presented. On the basis of these further insight into the interpretation of the characteristic length scale is sought.

6. Simulations

The simulations presented here follow the example from Hassanizadeh et al. [18], who apply the Richards equation with an extended $P_c(S_w)$ relationship in simulations of an imbibition process. We here simulate the same example solving the balance equations as given in Eqs. (9) and (10). A reference case with $\tau = 0$ will be compared to cases where the τ coefficient has a given magnitude.

Table 2 lists the porous medium and fluid properties as well as the parameters of the constitutive relationships for the simulations performed here. The wetting and non-wetting phases are water and gas (air), respectively. By setting the gas pressure at the boundaries equal to atmospheric pressure, the conditions of the Richards equation [38] are met where the gas pressure is constant. Here, the atmospheric reference pressure equals $P_n = 10^5$ Pa. The parameterisation of Van Genuchten [45] for the $P_c(S_w)$ relationship and the approach after Van Genuchten/ Mualem [32] for the $k_{r\alpha}(S_\alpha)$ relationships are employed here. Two cases are distinguished which differ in the magnitude of the intrinsic permeability.

Table 2
Fluid and porous medium properties for the imbibition example

Property	Value
Viscosity wetting phase μ_w	1.0×10^{-3} Pa s
Viscosity non-wetting phase μ_n	1.7×10^{-5} Pa s
Residual saturation wetting phase S_{wr}	2.8×10^{-1}
Porosity ϕ	3.7×10^{-1}
Residual saturation non-wetting phase S_{nr}	0
Van Genuchten α	3.4×10^{-4} 1/Pa
Van Genuchten n	2.0
Intrinsic permeability K	
1st case	9.4×10^{-10} m^2
2nd case	1.0×10^{-12} m^2

The simulations were carried out with the simulation toolbox MUFTE-UG using a finite volume space discretisation (BOX scheme, see [21]) and a fully implicit time stepping. The simulations are described in more detail in [29].

The initial and boundary conditions for the imbibition example are given in Fig. 5. In the y-direction the domain is discretised with 40 cells. As in MUFTE 1D simulations are not possible, the domain has a width of 0.1 m and a depth of 1 m. Initially, a wetting phase pressure of $P_w = 1900$ Pa and a non-wetting phase saturation of $S_n = 0.701$ are applied. For both fluid phases Dirichlet boundary conditions are chosen at the opposing ends of the domain. The wetting phase pressure is set to 1900 Pa at the right boundary and to 92642.5 Pa at the left boundary. This corresponds to $P_c = 7357.5$ Pa at the left boundary and $P_c = 98100$ Pa at the right boundary. This reduction in capillary and increase in wetting phase pressure compared to the initial conditions induces the wetting phase to infiltrate into the domain. The saturation of the non-wetting phase at the boundary corresponds to $S_n = 1.0 - S_w(P_c)$.

All in all, five simulations of the imbibition process were carried out:

(1) First case with $K = 9.4 \times 10^{-10}$ m^2 (see left Fig. 6)
   - reference, $\tau = 0$
   - $\tau = 10^5$ Pa s
   - $\tau = 10^7$ Pa s
(2) Second case with $K = 1.0 \times 10^{-12}$ m^2 (see right Fig. 6)
   - reference, $\tau = 0$
   - $\tau = 10^7$ Pa s

The characteristic flow velocity for the first case was estimated on the basis of the simulation results to equal

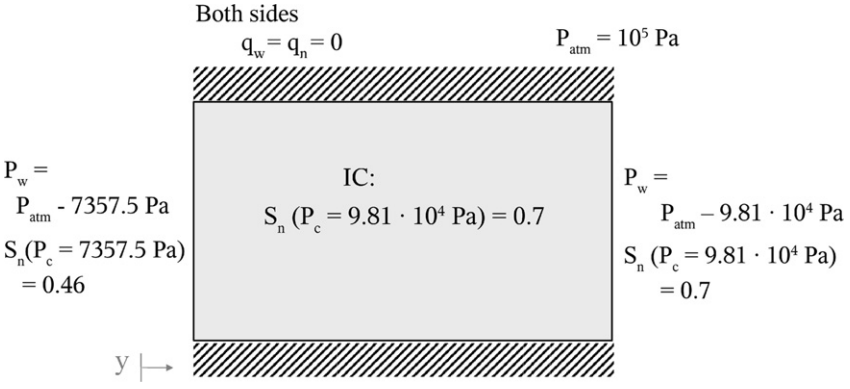

Fig. 5. Boundary and initial conditions for the first imbibition example.

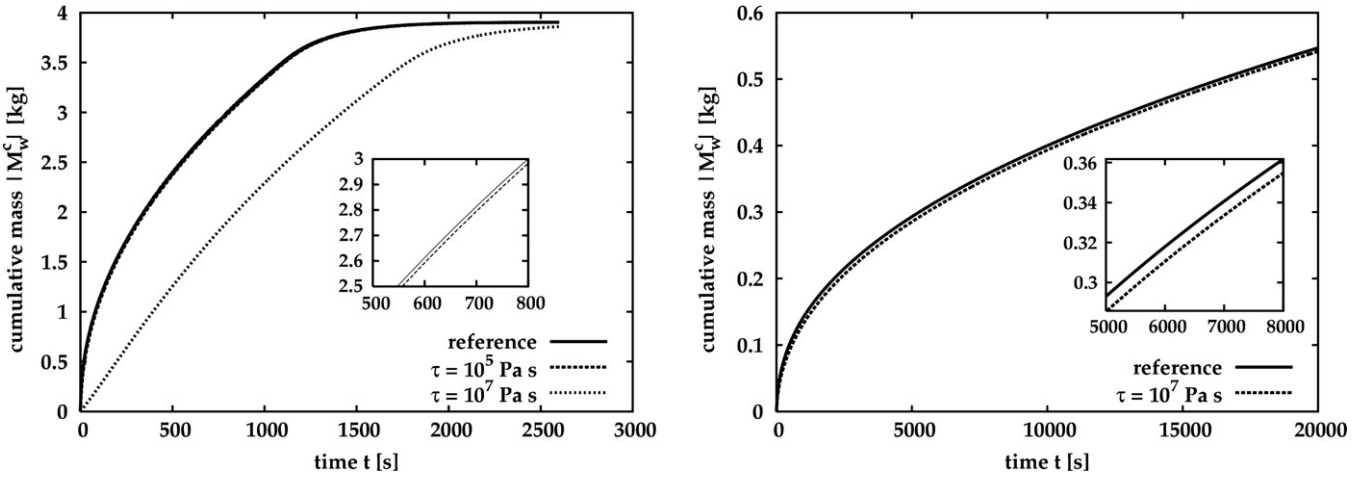

Fig. 6. Norm of the cumulative mass of wetting phase $M_w^c(t)$ from simulations of the first case ($K = 9.4 \times 10^{-10}\,\mathrm{m}^2$, left) and the second case ($K = 1.0 \times 10^{-12}\,\mathrm{m}^2$, right).

$u_c = 10^{-5}$ m/s. The Reynolds number thus remains less than one ($\mathrm{Re} = 7.8 \times 10^{-3}$) using the seepage velocity and the representative pore diameter. In the second example, an even smaller intrinsic permeability and thus smaller characteristic flow velocity $u_c = 10^{-7}$ m/s results in a Reynolds number much smaller than one.

The norm of the cumulative mass of wetting phase inside the domain for the simulations of the first case is compared (see left Fig. 6). This illustrates that the coefficient needs to exceed a threshold value to influence the simulation results noticeably (assuming that all other settings such as the boundary conditions remain the same). A difference between the reference case and $\tau = 10^5$ Pa s can only be seen when zooming into the graph (or comparing the actual values). For the chosen example, the inclusion of the extended $P_c(S_w)$ relationship results in a retardation of the infiltration of water into the domain for $\tau = 10^7$ Pa s.

For the second case the intrinsic permeability was decreased (see right Fig. 6), resulting in only a slight influence on the solution even if the large τ value of $\tau = 10^7$ Pa s is applied.

We now check whether our simulation results can be used to test our interpretations of the new dimensionless numbers and the characteristic length as presented in the previous section. It should be pointed out that for an assessment of the dynamic capillary forces only times smaller than $t < 2500$ s are of interest for the first case. At times much larger than this, steady-state conditions are reached and the dynamic force does not need to be taken into account.

Dy as well as DyC are calculated for the imbibition simulations described above (see Table 3). The characteristic capillary pressure is obtained from the equilibrium $P_c(S_w)$ relationship at $P_c(S_e = 0.5)$. For the characteristic length scale either the system length, the front width or the representative pore diameter are employed. As in this case the capillary rise with $l_c = 0.52$ m is of the same order of magnitude as the system length the dimensionless numbers are only calculated for the latter.

In the previous section it was suggested to calculate l_c after Eq. (29) having made use of the fractional flow formulation. Application of this formula to the presented cases results in a characteristic length that is by orders of magnitude larger than the system length. In such cases we suggested to alternatively use the system length. As a consequence, as we already use the system length, a

Table 3
Dimensionless numbers Dy and DyC for the two imbibition cases

Dimensionless number	System length $l_c = 0.6$ m	Front width $l_c = 0.1$ m	Pore diameter $l_c = 2.7 \times 10^{-4}$ m
1st *case*			
Dy [–] for $\tau = 10^5$ Pa s	7.1×10^{-1}	2.6×10^{1}	3.1×10^{6}
Dy [–] for $\tau = 10^7$ Pa s	7.1×10^{1}	2.6×10^{3}	3.1×10^{8}
DyC [–] for $\tau = 10^5$ Pa s	8.9×10^{-4}	5.3×10^{-3}	1.9×10^{0}
DyC [–] for $\tau = 10^7$ Pa s	8.9×10^{-2}	5.3×10^{-1}	1.9×10^{2}
			Pore diameter $l_c = 9.3 \times 10^{-6}$ m
2nd case			
Dy [–]	7.6×10^{-2}	2.7×10^{0}	3.1×10^{8}
DyC [–]	8.9×10^{-4}	5.3×10^{-3}	5.7×10^{1}

For the calculation of DyC: 1st case $u_c = 10^{-5}$ m/s, 2nd case $u_c = 10^{-7}$ m/s; $P_{cc} = P_c^e(S_e = 0.5) = 5.1 \times 10^3$ Pa; for other parameters see Table 2.

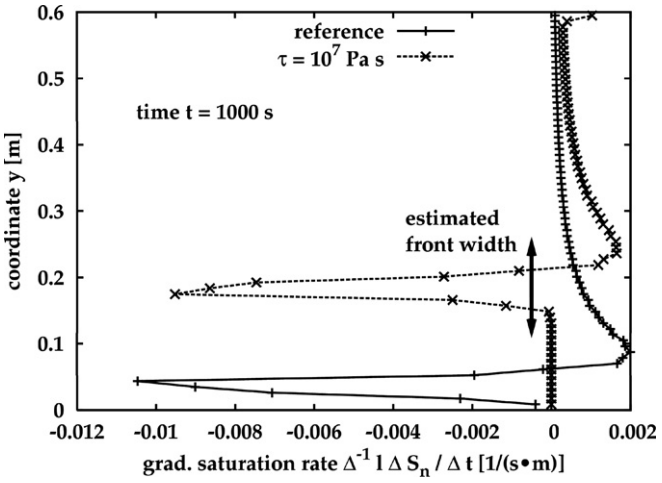

Fig. 7. Gradient of the rate of change of saturation at $t = 1000$ s for the first imbibition case.

different approach for the determination of the front width is applied here. It is estimated using the gradient of the saturation rate at $t = 1000$ s (calculated in a post processing step for each node, see Fig. 7). The part of the domain where the gradient runs through a minimum is assumed to correlate with the front width. The motivation for using this gradient was that it appears as an additional term in the balance equation of the non-wetting phase when the extended $P_c(S_w)$ relationship is applied as a closure assumption. Note that the front width should relate to a transient process and will therefore change in time. Thus a characteristic front width needs to be identified, similar to determining a characteristic capillary pressure with capillary pressure also changing with time during the considered process.

Application of the system length or the front width leads to satisfying results for the presented cases. Using the system length (or in this case the capillary rise) for calculating Dy the right prediction would be made that the solution is influenced by the inclusion of the extended $P_c(S_w)$ relationship with the high τ value. In the first case also the slight influence for the example with the lower τ value is indicated by Dy near to one. However, in the second case the perhaps negligible influence on the solution is rather underestimated. Application of the front width yields slightly more satisfying results as the small influence on the solution as depicted by the zooms in Fig. 6 is clearly predicted. The front width can be interpreted in a physical sense. Assuming that steep fronts are encountered in fast processes and broad fronts in slow processes, the number Dy would then predict correctly that for slow processes the dynamic capillary force does not need to be taken into account. As a consequence, using this interpretation of l_c, also the flow velocity enters indirectly into the calculation of the dimensionless number Dy.

When a representative pore diameter is inserted into Dy the influence on the solution is overestimated for the first case using $\tau = 10^5$ Pa s and the second case. We thus suggest not to use a representative pore diameter for the calculation of the dimensionless numbers Dy and DyC. Although, e.g. for a bundle of tubes the permeability can be upscaled from the pore to the Darcy scale on the basis of the pore diameters, in natural porous media the correlation between pore diameter (distribution) and permeability cannot be described by simple functions. The permeability can only be calculated in case also parameters such as the connectivity of the pores are known. By abstaining from using a representative pore diameter scales are not confounded.

Neglecting the magnitudes of the dimensionless number DyC for the pore diameter the choice of system length or front width both predict that equilibrium capillary forces dominate the dynamic capillary forces. As a consequence, the number DyC on its own could not give an assessment as to whether the solution would be influenced by the dynamic $P_c(S_w)$ relationship or not.

Closing this section we would like to point out that with the dimensionless number Dy only a quantitative assessment of the influence stemming from the extended $P_c(S_w)$ relationship can be given. Van Duijn et al. [44] and DiCarlo [14] have shown that consideration of the extended $P_c(S_w)$ function can lead to non-monotonous solutions.

7. Conclusions

The conclusions from the dimensional analysis can be summarised as follows:

- From the dimensional analysis of the two-phase balance equations including an extended $P_c(S_w)$ relationship, a new dimensionless number Dy evolves which quantifies the ratio of the dynamic capillary effect to viscous influences. Division of Dy by the capillary number Ca and the gravitational number Gr yields DyC, the ratio of dynamic to capillary equilibrium forces, and DyG, the ratio of dynamic to gravitational effects respectively.
- The assessment of the dominating terms in the balance equations on the basis of the dimensionless numbers alone presumes that the dimensionless gradients of the pressures and the saturation rate scale on the same order of magnitude. This can only be ensured if the values of the characteristic magnitudes are chosen accordingly. If such a choice is not possible the products of the dimensionless numbers with the dimensionless gradients need to be considered and compared.
- Looking at the dimensionless numbers independently, it may be stated that under the assumption that the coefficient τ is a constant the importance of the dynamic capillary force diminishes with increasing length scale with relation to equilibrium capillary, viscous and gravitational effects.
- If the characteristic length scale is assumed to be the system length, dynamic effects might play a role especially in laboratory experiments (e.g. for parameter identification) and small scale applications (e.g. filters) where large rates of change of saturation occur.

- The influence of the dynamic forces increases with increasing characteristic flow velocity when transient processes are considered.
- Consideration of the extended $P_c(S_w)$ relationship may be important for porous media with high permeability, small entry pressure and high coefficient tau when systems with a small characteristic length (e.g. steep font) and small characteristic time scale are under investigation.
- If the initial and boundary conditions do not change, the dimensionless number Dy gives a good estimation of the possible influence of the dynamic term in comparison to a reference case with $\tau = 0$ in case an appropriate characteristic length scale is chosen. As appropriate we consider e.g. the front width as it captures the influence stemming from the process as well as porous media parameters such as the $P_c(S_w)$ relationship.
- The range in which the dynamic effects might play a role is limited by at least two factors,
  - the smallest length scale possible for establishing an REV for the balance equations and the properties of the porous medium and
  - the maximum flow velocity (of a transient process where it may be assumed that the maximum flow velocity correlates with the rate of change of saturation) where the Reynolds number does not exceed unity. In most applications concerning subsurface hydrosystems, the Reynolds number does not exceed this limit.

In brief, the influence of the dynamic capillary force declines with increasing length scale (of either the system or the front width) and decreasing flow velocity presuming that τ is a constant.

The dimensionless analysis is based on the assumption that the coefficient τ is independent of scale. Dahle et al. [12] propose that τ scales with length squared for a large range of water saturations. These results were confirmed by Gielen et al. [17] and Manthey et al. [30]. As a consequence, the ratios of the dynamic capillary to the viscous and gravitational forces would not depend on the length scale, as l_c^2 then cancels out and only the constant part of τ remains in the dimensionless numbers. If this relation is inserted into Eq. (23), the dynamic capillary force still increases with length scale in comparison to the equilibrium capillary effects then constant over all length scales. Relating τ instead of to the system length to a front width, as suggested by Dahle et al. [12], also raises questions. If the coefficient scales directly with length squared, it is then large for a broad front width and small for steep fronts. This introduces a dependence on the flow processes assuming that steep fronts are encountered in processes with high flow velocities and broad fronts are related to small flow velocities. Additionally, having a large coefficient for slow processes violates the assumption that in the limit of capillary dominated flow dynamic effects do not need to be taken into account.

Acknowledgements

We would like to thank Dani Or, Lausanne for his very helpful comments and discussions of the manuscript. Moreover, the reviews of three anonymous reviewers are highly appreciated. This work was supported by the Deutsche Forschungsgemeinschaft (DFG) within the project First-principle based Modelling of Transport in Unsaturated Media under the Grant He 2531/5-1.

References

[1] Anton L, Hilfer R. Trapping and mobilisation of residual fluid during capillary desaturation in porous media. Phys Rev E 1999;59(6):6819–23.
[2] Barenblatt GI, Azorero JG, De Pablo A, Vazquez JL. Mathematical model of non-equilibrium water–oil displacement in porous strata. Appl Anal 1997;65:19–45.
[3] Barenblatt GI, Gilman AA. Nonequilibrium counterflow capillary impregnation. J Eng Phys 1987;52:335–9.
[4] Barenblatt GI, Patzek TW, Silin DB. The mathematical model of non-equilibrium effects in water–oil displacement. SPE/DOE 13th symposium on improved oil recovery, vol. SPE 75169. USA: Tulsa; 2002.
[5] Bialas Z, Kleczkowski AS. O prezdydatnosciniektorych wzorow empirycznych dla okreslenia wspo czynnika filtracji k, Archiwum Hydrotechniki 1970;407–17 [English summary on page 417].
[6] Blake TD, Bracke M, Shikhmurzaev YD. Experimental evidence of nonlocal hydrodynamic influence on the dynamic contact angle. Phys Fluids 1999;11(8):1995–2007.
[7] Bottero S, Hassanizadeh SM, Kleingeld PJ, Bezuijen A. Experimental study of dynamic capillary pressure effect in two-phase flow in porous media. In: Binning PJ, Engesgaard PK, Dahle HK, Pinder F, Gray WG, editors. Conference proceeding, XVI international conference in computational methods in water resources, June 19–22, 2006, Copenhagen, Denmark, 2006.
[8] Brooks RH, Corey AT. Hydraulic properties of porous media. Hydrology papers, vol. 3. Fort Collins: Colorado State University; 1964.
[9] Charbeneau RJ. Groundwater hydraulics and pollutant transport. Upper Saddle River: Prentice Hall; 2000.
[10] Corey AT. Mechanics of immiscible fluids in porous media. Water Resources Publications; 1994.
[11] Cuesta C, van Duijn CJ, Hulshof J. Infiltration in porous media with dynamic capillary pressure: travelling waves. Euro J Appl Math 2000;11:381–97.
[12] Dahle HK, Celia MA, Hassanizadeh SM. Bundle of tubes model for calculating dynamic effects in the capillary pressure–saturation relationship. In: Das DB, Hassanizadeh SM, editors. Upscaling multiphase flow in porous media. Springer; 2005. p. 5–22.
[13] Davidson JM, Nielsen DR, Biggar JW. The dependence of soil water uptake and release upon the applied pressure increment. Soil Sci Soc Am Proc 1966;30:298–304.
[14] DiCarlo DA. Modelling observed saturation overshoot with continuum additions to standard unsaturated theory. Adv Water Resources 2005;28:1021–7.
[15] Fermigier M, Jenffer P. Experimental investigation of the dynamic contact angle in liquid–liquid systems. J Colloid Interface Sci 1991;146:226–41.
[16] Friedman SP. Dynamic contact angle explanation of flow rate-dependent saturation–pressure relationships during transient liquid

flow in unsaturated porous media. J Adhesion Sci Technol 1999;13(12):1495–518.
[17] Gielen T, Hassanizadeh SM, Leijnse A, Nordhaug HF. Dynamic effects in multiphase flow: a porscale network approach. In: Das DB, Hassanizadeh SM, editors. Upscaling multiphase flow in porous media. Springer; 2005. p. 217–36.
[18] Hassanizadeh SM, Celia MA, Dahle HK. Dynamic effect in the capillary pressure–saturation relationship and its impact on unsaturated flow. Vadose Zone Hydrol 2002;1:38–57.
[19] Hassanizadeh SM, Gray WG. Mechanics and thermodynamics of multiphase flow in porous media including interphase boundaries. Adv Water Resources 1990;13(4):169–86.
[20] Hassanizadeh SM, Oung O, Manthey S. Laboratory experiments and simulations on the significance of non-equilibrium effect in capillary pressure–saturation relationship. In: Schanz T, editor. Unsaturated soils: experimental studies, proceedings of the international conference 'from experimental evidence towards numerical modeling of unsaturated soils' in Weimar, Germany, September 18–19, 2003, vol. I. Springer proceedings in physics, vol. 93. Springer; 2005. p. 3–14.
[21] Helmig R. Multiphase flow and transport processes in the subsurface. Springer; 1997.
[22] Hilfer R. Transport and relaxation phenomena in porous media. Adv Chem Phys 1996;XCII:299–424.
[23] Hilfer R, Helmig R. Dimensional analysis and upscaling of two-phase flow in porous media with piecewise constant heterogeneities. Adv Water Resources 2004;27(10):1033–40.
[24] Hilfer R, Øren PE. Dimensional analysis of pore scale and field scale immiscible displacement. Transport Porous Media 1996;22:53–72.
[25] Kalaydjian F. A macroscopic description of multiphase flow in porous media involving spacetime evolution of fluid/fluid interface. Transport Porous Media 1987;2:537–52.
[26] Kalaydjian F. Dynamic capillary pressure curve for water/oil displacement in porous media: theory vs. experiment. Soc Petrol Eng SPE 1992;24813:491–506.
[27] Kneale WR. Observations of the behaviour of large cores of soil during drainage and the calculation of hydraulic conductivity. J Soil Sci 1985;36:163–71.
[28] Lenhard RJ, Parker JC, Mishra S. On the correspondence between Brooks-Corey and van Genuchten models. J Irrigation Drain Eng 1989;155(4):744–51.
[29] Manthey S. Two-phase flow processes with dynamic effects in porous media – parameter estimation and simulation. PhD thesis, Institut für Wasserbau, Fakultät Bau- und Umweltingenieurwissenschaften, Universität Stuttgart; 2006.
[30] Manthey S, Hassanizadeh SM, Helmig R. Macro-scale dynamic effects in homogeneous and heterogenous porous media. Transport Porous Media 2005;58:121–45.
[31] Manthey S, Hassanizadeh SM, Oung O, Helmig R. Dynamic capillary pressure effects in two-phase flow through heterogeneous porous media. In: Miller Cass T, Farthing MW, Gray WG, Pinder GF, editors. Proceedings of the XV international conference on'computational methods in water resources, June 13–17, 2004, vol. I. Chapel Hill, (NC, USA): Elsevier; 2004. p. 631–44.
[32] Mualem Y. A new model for predicting the hydraulic conductivity of unsaturated porous media. Water Resources Res 1976;12(3):513–22.
[33] Nieber JL, Dautov RZ, Egorov AG, Sheshukov AY. Dynamic capillary pressure mechanism for instability in gravity-driven flows: review and extension to very dry conditions. In: Das DB, Hassanizadeh SM, editors. Upscaling multiphase flow in porous media. Springer; 2005. p. 147–72.
[34] Nordbotten JM, Celia M, Dahle HK, Hassanizadeh SM. Interpretation of macro-scale variables in Darcy's law, Water Resources Res 2007;43:W08430. doi:10.1029/2006WR005018 .
[35] O'Carroll DM, Phelan TJ, Abriola LM. Exploring dynamic effects in capillary pressure in multistep outflow experiments. Water Resources Res 2005;41:W11419. doi:10.1029/2005WR004010.
[36] Oung O, Hassanizadeh SM, Bezuijen A. Two-phase flow experiments in a geocentrifuge and the significance of dynamic capillary pressure effect. J Porous Media 2005;8(3):247–57.
[37] Pankow JF, Cherry JA. Dense chlorinated solvents and other DNAPLs in groundwater. Portland, (Oregon, USA): Waterloo Press; 1996.
[38] Richards LA. Capillary conduction of liquids through porous medium. Physics 1931:318–33.
[39] Schultze B, Ippisch O, Huwe B, Durner W. Dynamic nonequilibrium during unsaturated water flow. In Leija FJ, van Genuchten MTh, Wu L, editors. Proceedings of the international workshop on characterization and measurement of the hydraulic properties of unsaturated porous media, vol. 2, University of California. Riverside, CA, USA, October 22 – 24, 1997. p. 877–92.
[40] Stauffer F. Time dependence of the relations between capillary pressure, water content and conductivity during drainage of porous media. in: On scale effects in porous media, Thessaloniki, Greece, 1978. IAHR.
[41] Topp GC, Klute A, Peters DB. Comparison of water content-pressure head data obtained by equilibrium, steady-state, and unsteady-state methods. Soil Sci Soc Am Proc 1967;31:312–4.
[42] Ursino N, Gimmi T, heterogeneity Combined effect of. anisotropy and saturation on steady state flow and transport: structure recognition and numerical simulation. Water Resources Res 2004;40:W01514.
[43] Vachaud G, Vauclin M, Khanji D, Wakil M. Effects of air pressure on water flow in an unsaturated stratified vertical column of sand. Water Resources Res 1973;9(1):160–73.
[44] van Duijn CJ, Peletier LA, Pop IS. A new class of entropy solutions of the Buckley–Leverett equation. SIAM J Math Anal 2007;39(2):507–36.
[45] Van Genuchten MT. A closed-form equation for predicting the hydraulic conductivity of unsaturated soils. Soil Sci Soc Am J 1980;44:892–8.
[46] Van Genuchten MT, Schaap MG, Mohanty BP, Simunek J, Leij FJ. Modeling flow and transport processes at the local scale. In: Feyen J, Wiyo K, editors. Modelling of transport processes in soils. Belgium: Leuven; 1999. p. 23–45.
[47] Watson KK. Water content-pressure head relationship. Soil Sci Soc Am Proc 1968;32:892.
[48] Weislogel MM. Steady spontaneous capillary flow in partially coated tubes. AIChE J 1997;43(3):645–54.
[49] Wiedemeier TH, Rifai HS, Newell CJ, Wilson JT. Natural attenuation of fuels and chlorinated solvents in the subsurface. USA: John Wiley & Sons; 1999.
[50] Wildenschild D, Hopmanns JW, Simunek J. Flow rate dependence of soil hydraulic characteristics. Soil Sci Soc Am J 2001;65:35–48.